Diyala Journal of Engineering Sciences

Journal homepage: https://djes.info/index.php/djes

ISSN: 1999-8716 (Print); 2616-6909 (Online)

# Green Synthesis, Characterization and Evaluation of Biological Activities of Ag-Mno Nanocomposites from Cyttaranthus Congolensis

Giresse N. Kasiama[1*], Carlos N. Kabengele[1], Jason T. Kilembe[1], Jules M. Kitadi[3], Michel Mifundu[1], Jean Paul Ngbolua[2], Damien S.T. Tshibangu[1], Dorothée D. Tshilanda[1] and Pius T. Tshimankinda[1]

1 Department of Chemistry, Faculty of Sciences, University of Kinshasa, BP 190, Kinshasa XI, Democratic Republic of Congo.
2 Department of Biology, Faculty of Sciences, University of Kinshasa, BP 190, Kinshasa XI, Democratic Republic of Congo
3 Faculty of Sciences, University of Kikwit, BP76, Kikwit, Democratic Republic of Congo.

**ARTICLE INFO**

***Article history:***
Received May 3, 2023
Revised July 11, 2023
Accepted July 13, 2023
Available online September 1, 2023

***Keywords:***
Cyttaranthus congolensis
Silver
Manganese nanocomposites

**ABSTRACT**

This study consists of biogenic synthesis of Ag-MnO nanocomposite whose aqueous extract from *Cyttaranthus congolensis* was used as a reducer and stabilizer. The characterization of these particles by visible UV spectroscopy made it possible to identify the band linked to the surface plasmon resonance located around 380 nm. X-ray Diffraction and Fluorescence made it possible to determine the presence of particles of formula Ag 0.21 Mn 0.28 O having crystallized in a Monoclinic system (a= 5.8517 Å, b = 3.4674 Å, c = 5.4838 Å and β = 107.663°). A spherical morphology was determined by Scanning Electron Microscopy (SEM). The haemolytic activity carried out on human blood made it possible to conclude that Ag-MnO nanocomposites are not toxic to human blood. Moreover, these particles showed good antibacterial activity against gram-positive and gram-negative strains of bacteria. Promising results on anthelminthic activity of Ag-MnO nanocomposites against several pathogenic helmints were reported in this study. Besides antibacterial and antihelmintic activities, Ag-MnO nanocomposites also exhibited good anti-inflammatory and antioxidant activity.

## 1. Introduction

Nanotechnologies and nanosciences represent a new "world" where matter has very different properties from what it has on a larger or macroscopic scale. Due to their varied and often novel properties, bimetallic nanomaterials have diverse potentialities and their uses open up multiple perspectives in many sectors of activity such as environment, health, automotive, construction, agri-food and electronics. Their properties are generally a synergistic combination of two metals which constitute them. Two approaches (bottom-up and top-down) are generally used in the preparation of nanoparticles [1-4].

In top-down approach, we start from a large structure that is undersized, until reaching nanometric dimensions while the bottom-up approach, the production of nanoparticles is done by assembling atom by atom or molecule by molecule [5]. These two approaches use physical and chemical methods whose development for nanoparticles production on large scale generally comes up against certain constraints such as energy consumption, low yield, use of harmful organic solvents as stabilizers, production of intermediates and toxic waste at the base of environmental

* Corresponding author.
E-mail address: giresse.kasiama@unikin.ac.cd
DOI: 10.24237/djes.2023.16303

pollution. In addition, Nanoparticles (NPs) produced by chemical methods keep the molecules used for stabilization on their surfaces, thus limiting their uses in the medical and pharmaceutical fields because stabilizers define nanoparticles solubility and give them certain surface properties [6-8].

In this context, many studies are currently focused on the use of biological methods to produce nanoparticles. Biological synthesis involves the use of extracts of living beings (plants, microorganisms) as reducing and stabilizing agents, the first study carried out in this direction was the preparation of silver nanoparticles using microorganisms [9]. Recent studies have reported the use of plant extracts in the preparation of metallic nanoparticles.

Indeed, polyphenols (flavonoids, saponins…), alkaloids, proteins, phenolic acids, sugars, tepenoids contained in various parts of plants play a key role in the reduction and stabilization of metal ions to produce nanoparticles. Thus, in addition to protecting the environment and human health by reducing the use of toxic chemicals. The use of plant extracts reduces number of steps, energy, preparation time and NPs retain active chemical molecules on their surfaces improving their efficacy and properties in medical and pharmaceutical field [10-12].

Among different types of metallic nanoparticles, silver and manganese attracted attention of many researchers because of their multiple applications in various scientific fields. These nanoparticles have been widely used as antibacterial, antiheminthic, antioxidant, optical, photovoltaic and photocatalytic agent [13-18].

However, there is no data on the association of these two metals in the form of nanocomposites using *Cyttaranthus congolensis* extract. Indeed, this combination generally leads to the improvement of the properties of the material following a synergistic effect of their properties. Thus, this study is part of the search for a new material synthesized by green methods and having interesting biological properties.

In the present study, Ag-MnO nanocomposites were synthesized using the aqueous extract of *Cyttaranthus congolensis* leaves. This plant is edible and belongs to the family of Euphorbiaceae. It's used as tea in traditional medicine to relieve sickle cell disease and is rich in polyphenolic and triterpenic compounds that can play the role of reducer and stabilizer in Ag-MnO nanocomposites preparation. Several characterization techniques were used to confirm the synthesis of these particles including UV-visible spectroscopy for Surface Plasmon Resonance band, XRD analysis is used to study the crystal system and lattice parameters, while the X-ray fluorescence analysis is used to study the chemical composition. Scanning Electron Microscopy (SEM) was performed to determine particle morphology. Antibacterial activity of these nanocomposites was evaluated using diverse bacterial strains such as Eschierichia coli, Staphylococcus aureus and Pseudomonas aeruginosa.

## 2. Materials and methods

### *2.1.Materials*

In this study, *Cyttaranthus congolensis* leaves were collected in Kwilu province, Democratic Republic of the Congo. The plant was identified in the herbarium of the National Institute for Agronomic Studies and Research (INERA) of the University of Kinshasa (UNIKIN). Five bacterial strains were used, including two gram-positive strains (Staphylococcus aureus ATCC 25923, Staphylococcus aureus ATCC 29213) and three gram-negative strains (Eschierichia coli ATCC 25922, Escherichia coli ATCC 35 218 and Pseudomonas aeruginosa ATCC 25783).

These strains were provided by the microbiology laboratory of the Faculty of Pharmaceutical Sciences of the University of Kinshasa. The earthworm specimens were collected on the Keni River in Kinshasa. Manganese sulfate ($MnSO_4$), silver nitrate ($AgNO_3$), and resazurin were from Sigma-Aldrich. Cyanomethemoglobin (CMH) reagents and hemoglobin standards were purchased from StanBio. Two culture media, Muller Hinton agar (for the subculture of bacterial strains) and Muller Hinton broth (for the sensitivity test), were provided by the microbiology laboratory

of the Faculty of Pharmaceutical Sciences of the University of Kinshasa. Bi-distilled water was used in the preparation of the solutions.

### *2.2.Chemical screening in solution and TLC*

Fresh *Cyttaranthus congolensis* leaves have been washed several times with water to remove impurities and dust, dried, and then reduced to powder using a Sinbo-type grinder. Phytochemical screening in solution was carried out following the procedure described by Ngoyi et al. [19]. A standard protocol based on spot color observation to identify different secondary metabolites was used for thin layer chromatography [20].

### *2.3. Assay of secondary metabolites*

The total polyphenol content of *Cyttaranthus congolensis* extract was determined using the Folin-Ciocalteu method [21]. The determination of total flavonoids and anthocyanins was carried out following the method described by Kasiama et al. [20].

### *2.4. Preparation of extracts*

10g of *Cyttaranthus congolensis* powder were macerated in 100 ml of bidistilled water for 24 hours with stirring at room temperature. The aqueous extract was obtained after filtration with filter paper (Whatman No. 42) and stored in an airtight bottle at 6°C.

### *2.5. Biosynthesis of Ag-MnO nanocomposites*

The experimental procedure described by Kabengele was used for the biogenic synthesis of Ag-MnO nanocomposites [22].

The aqueous extract of *Cyttaranthus congolensis* reacted with two equal concentrations of 0.1N Magnesium sulfate ($MnSO_4$) and 0.1N silver nitrate ($AgNO_3$) solutions under thermal stirring at 60°C and 1000 rpm. After 30 minutes of experiment, the color change of the solution from yellow to dark brown shows the beginning of metal precipitation in the form of composite nanoparticles. A few quantities of Ag- MnO nanoparticles synthesized were kept for Uv-visible spectroscopy measurement. After 2 hours of reaction, Ag-MnO obtained were collected by centrifugation at 4000 rpm for 15 minutes, then washed with distilled water and dried at 100° C and stored for characterizations.

### *2.6. Characterization of Ag-MnO nanocomposites*

The synthesized Ag-MnO nanocomposites were characterized using various spectroscopic methods. UV-visible spectra were recorded using JENWAY 7315 UV-visible spectrophotometer. The particle morphology was determined by TESCAN Lyra 3 Scanning Electron Microscope. To determine crystal structure and chemical composition of nanocomposites, X-ray diffraction patterns were obtained from X-ray diffractometer (PHYWE 4.0) equipped with CuKα radiation source (λ = 1.5406 Å) and X-ray fluorescence.

### *2.7. Antibacterial activity*

The antibacterial activity was carried out using microdilution method on liquid medium (Muller-Hinton medium) using 96-well microplates [23].

### *2.8. Antioxidant activity*

The antioxidant activity of Ag-MnO nanocomposites was evaluated using DPPH test according to the method used by Kasiama [20].

### *2.9. Anthelmintic activity*

The anthelmintic activity of Ag-MnO nanocomposites was evaluated according to the method described by Kabengele [24].

### *2.10. Anti-inflammatory activity*

In vitro Anti-inflammatory activity was evaluated according protein denaturation method (Albumin) described by Kumari [25].

### *2.11. Antihemolytic activity*

The test presented here is an adaptation of existing standard F-7560026, which is based on colorimetric detection of red-colored cyanomethemoglobin in solution [26].

## 3. Results and discussion

### *3.1. Phytochemical screening and TLC*

Various chemical groups were identified in *Cyttaranthus congolensis* leaves (polyphenols, alkaloids, triterpenoids, and steroids), while saponins were absent. TLC images confirmed the presence of triterpenes, anthracene derivatives, flavonoids, alkaloids, and coumarins, as presented in the figures below.

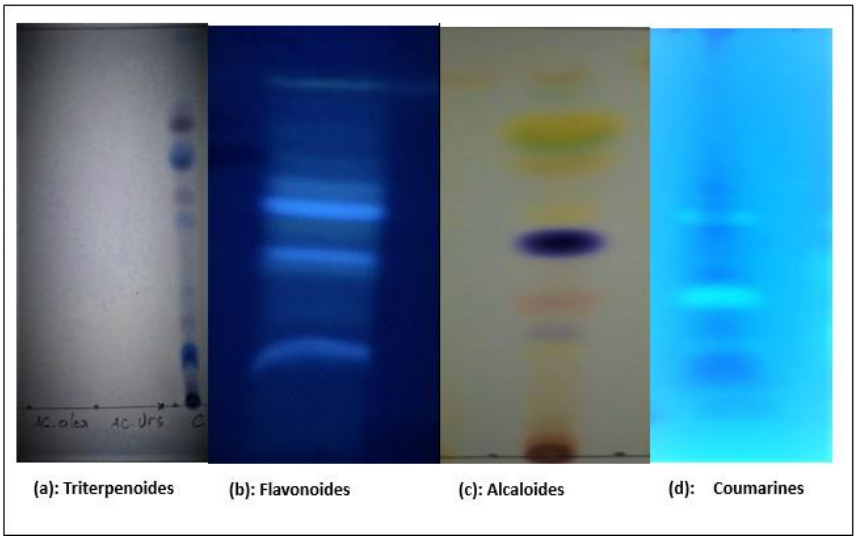


**Figure 1.** CCM images of triterpenoids (a), Flavonoids (b), Alcaloids (c) Coumarins (d)

Figure 1a above gives the spots corresponding to triterpenoids in *Cyttaranthus congolensis*, revealed by brown colored spots after development with sulfuric anysaldehyde and heating for 10 minutes. The chromatogram in Figure 1b confirmed the presence of flavonoids by blue spots after development under a UV lamp. The presence of alkaloids was revealed by yellow-colored spots after revelation with 5% sodium nitrite solution, as shown in figure 1c above. Coumarins on chromatoplate of Figure 1d showed blue- and purple-colored spots after spraying 10% ethanolic KOH and observing at 366 nm.

### *3.2.Secondary metabolites content*

#### *3.2.1. Polyphenols content*

Table 1 below presents the contents of total polyphenols, flavonoids, anthocyanins, condensed and hydrolyzable tannins in C. congolensis leaves.

**Table 1:** Content of total polyphenols, flavonoids, anthocyanins, condensed tannins and hydrolyzable tannins of C. congolensis

| Plants | Secondary metabolites | | | | |
|---|---|---|---|---|---|
| | **Total polyphenols (µg EAG /g)** | **Flavonoids (%)** | **Anthocyanins (%)** | **Condensed tannins (%)** | **Hydrolyzable tannins (%)** |
| *C. congolensis* | 458.220 ± 7.50 | 4.136±0.002 | 2.253 ± 0.004 | 3.431 ± 0.009 | 5.529 ± 0.005 |

The determination of total polyphenols, flavonoids, tannins and anthocyanins was carried out by UV-visible spectrophotometry. the results obtained show high levels of total polyphenols (flavonoids and tannins).

### *3.3.Synthesis*

The reaction medium changed from pale-yellow color to brown after 30 minutes as shown in figure 2 below. This color change is due to the excitation of surface plasmon vibrations in Ag-MnO nanocomposites [27].

**Figure 2.** Formation of nanoparticles in solution

### *3.4.Characterization of nanocomposites*

#### *3.4.1. UV-visible spectroscopy of nanocomposites*

The presence of Ag-MnO nanocomposites in solution was confirmed by UV-vis spectral analysis after 2 hours of contact, as presented in figure 3 below. A broad peak located between 350 and 400 nm, attributed to Ag-MnO nanoparticles was observed. This peak is related to Surface Plasmon Resonance, which has already been well documented for various metallic nanoparticles with sizes ranging from 2 nm to 100 nm [28].

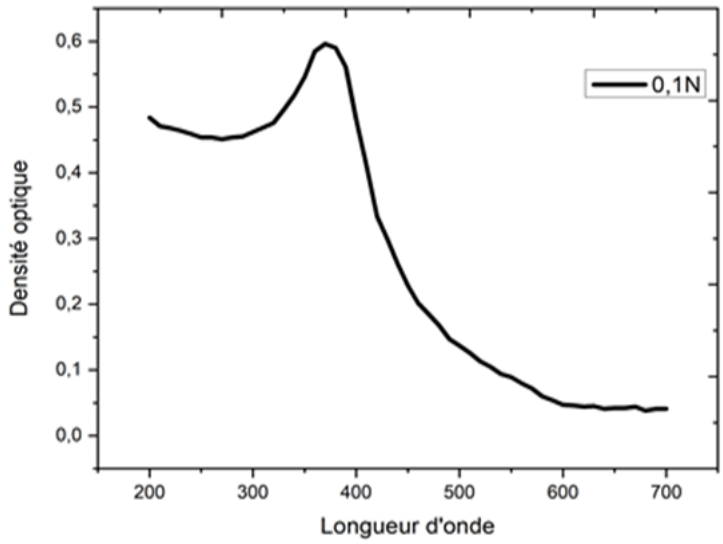


**Figure 3.** UV-visible spectrum of Ag -MnO nanocomposites

#### *3.4.2. Chemical composition of nanocomposite*

X-ray diffraction (XRD) studies of synthesized nanocomposites were performed at room temperature with a 4.0 PHYWE diffractometer using Cu Kα radiation. Figure 4 and Table 2 below show the XRD spectrum and its summary.

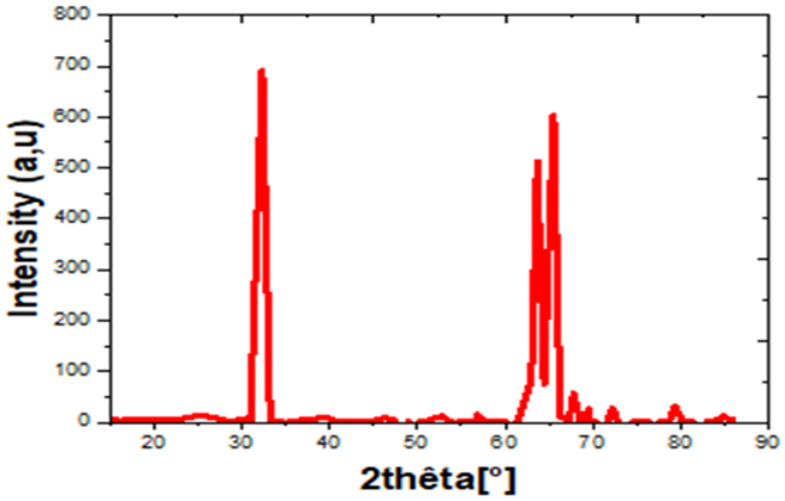


**Figure 4.** XRD diagram of synthesized Ag-MnO nanocomposites

**Table 2:** X-ray diffraction peak values of Ag-MnO nanocomposites

| No. | 2 theta[°] | [*A*] | $I/I_0$ | Accounts (peak area) | FWHM |
|---|---|---|---|---|---|
| **6** | 30.48 | 2.9300 | 904.12 | 3.83 | 1.3292 |
| **8** | 33.19 | 2.6971 | 972.91 | 1.12 | 0.3625 |
| **27** | 63.67 | 1.4604 | 455.74 | 2.05 | 1.4121 |
| **28** | 65.53 | 1.4234 | 556.67 | 2.39 | 1.3453 |

Table 2 represents four characteristic 2 theta peaks of (Ag-MnO) nanocomposites. It appears from these results that the composition of these particles is Ag 0.21 Mn 0.28 O which crystallized in a monoclinic system having as lattice parameters: a = 5.8517 A, b = 3.4674 A, c = 5.4838, and β = 107.663°, then the calculated density ϕ = 7.760 g/cm3. The average size determined via the Debye–Scherrer equation d = (kλ/βcosθ), where k is the Debye–Scherrer constant (0.89), λ is the wavelength of the X-ray (0.154 nm), β is the width of the maximum intensity peak at mid-height, d is the crystal thickness, and θ is the diffraction angle [29-31]. After calculation, the average size of the crystallites of the particles is of the order of 9.75 nm. The X-ray fluorescence spectrum in Figure 5 below allowed us to identify the presence of the metals silver (Ag-Kα and Ag-Kβ) and manganese (Mn-Kα and Mn-Kβ).

The X-ray fluorescence spectrum was recorded and is shown in Figure 5 below.

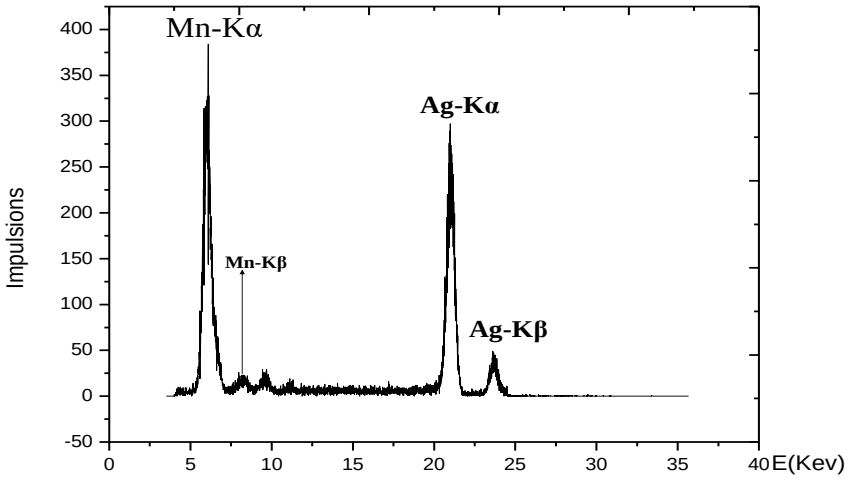


**Figure 5.** X-ray fluorescence spectrum of Ag-MnO nanoparticles

### *3.4.3. Morphology of nanocomposites*

The morphology of the synthesized Ag-MnO nanocomposites was determined using scanning electron microscopy (SEM). SEM images of Ag-MnO nanocomposites are shown in Figure 6 below.

Predominant spherical shape well-dispersed have been observed. A similar morphology has been reported in previous works [32].

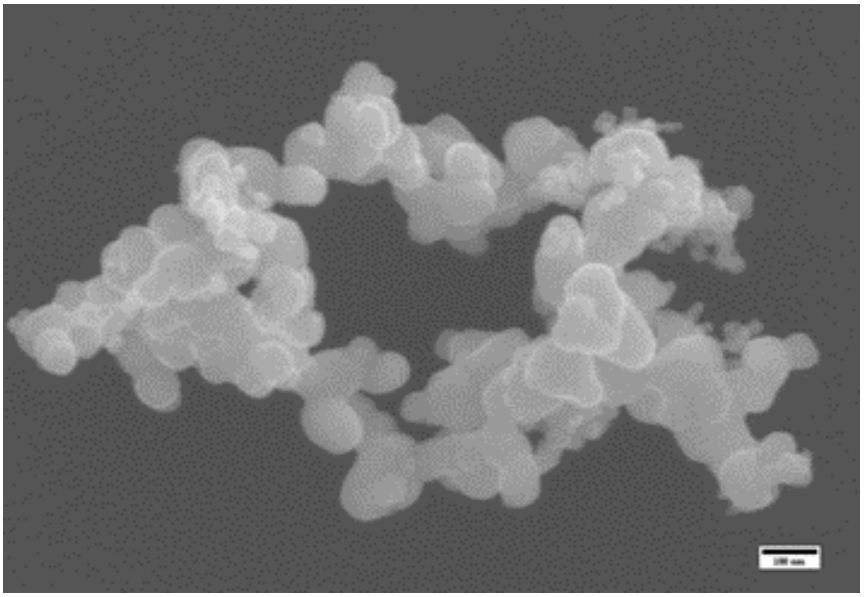

**Figure 6.** Morphology of Ag-MnO nanoparticles

### *3.5.Antibacterial activity*

It emerges from these results that the antibacterial effect is proportional to the concentration of Ag-MnO nanocomposites used. Indeed, the growth inhibition of Escherichia coli strains by different concentrations of Ag-MnONPs is greater compared to the other bacteria tested, minimum inhibitory concentrations (MIC) are obtained at 31.25 µg/mL for Escherichia strain coli ATCC 25922 and 62.5 µg/mL for Escherichia coli ATCC 35 218. Whereas Staphylococcus aureus strains (Staphylococcus aureus ATCC 25923

and Staphylococcus aureus ATCC 29213), the MIC is equal to 125 µg/mL for the two strains tested. For Pseudomonas aeruginosa ATCC 25783, Ag-MnO nanoparticles inhibited their development at MIC of 125 µg/mL. And with ciprofloxacin, which was considered the reference antibiotic, a total inhibition of bacteria growth is observed for MIC equal 0.25 µg/mL. Indeed, the Ag-MnO nanoparticles are very active against and exert a bactericidal effect on the all strains used in this study.

The mechanism of action of Ag-MnO nanoparticles comes from electrons pairs created on the surface of Ag-MnO NPs, that influence the oxidation-reduction reaction capable to generate reactive oxidizing species (ROS). In the presence of these free radicals, microorganisms' cells will be immediately destroyed via peptidoglycan and cell membranes, DNA, mRNA, ribosomes, and proteins. On the other hand, another mechanism has been proposed in which the bactericidal effect of nanoparticles is mainly explained by the rupture of the lipid double layer of bacteria, resulting in the leakage of cytoplasmic content [33,34].

**Table 3:** Different concentrations of Ag-MnO nanoparticles tested on Gram+ and Gram- bacteria

| **Bacteria** | **Concentrations (µg/mL) of Ag-MnONPs nanoparticles** | | | | | | | | | | | |
|---|---|---|---|---|---|---|---|---|---|---|---|---|
| | T+ | T- | 3.90625 | 7.8125 | 15,625 | 31.25 | 62.5 | 125 | 250 | 500 | 1000 | 2000 |
| *Staphylococcus aureus* ATCC 29213 | - | + | + | + | + | + | + | - | - | - | - | - |
| *Escherichia coli* ATCC 35 218 | - | + | + | + | + | + | - | - | - | - | - | - |
| *Pseudomonas aeruginosa* ATCC 25783 | - | + | + | + | + | + | + | - | - | - | - | - |
| *Staphylococcus aureus* ATCC 29213 | - | + | + | + | + | + | + | - | - | - | - | - |
| *Escherichia coli* ATCC 25922 | - | + | + | + | + | - | - | - | - | - | - | - |

Legend: +: growth of bacteria
-: no growth of bacteria

### *3.6.Anthelmintic activity*

Figure 7 gives the paralysis time of worms as a function of nanocomposites concentration.

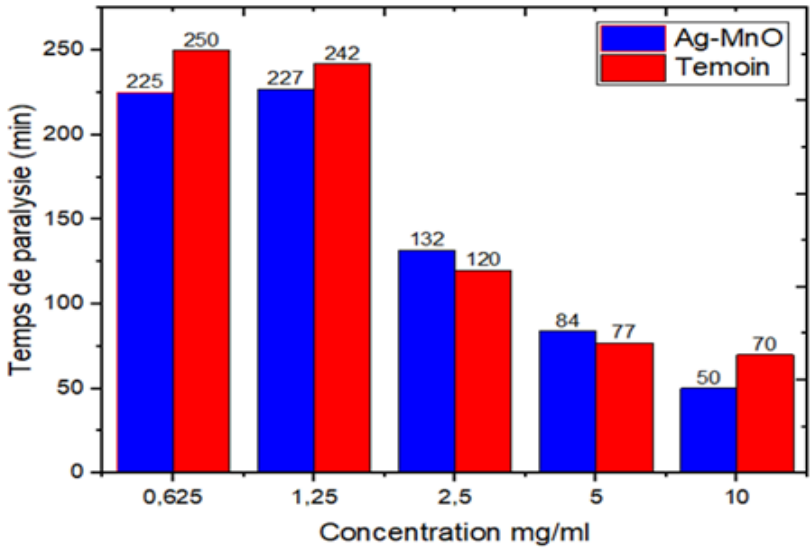


**Figure 7.** Paralysis time of worms as a function of drug concentration.

Worm paralysis time decreases when the concentration of Ag-MnO nanocomposites increases (from 0.625 to 10 mg/mL). At a high dose (10 mg/mL), this time decreases approximately 4 to 5 times, depending on the case.

Figure 8 gives the earthworm mortality rate as a function of the concentration of Ag-MnO nanocomposites.

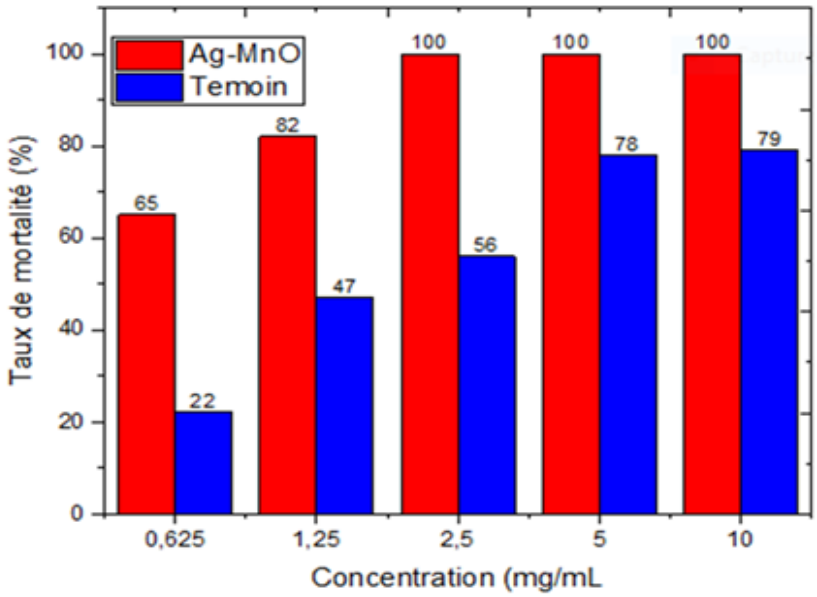


**Figure 8.** Worm mortality rate as a function of Ag-MnO nanocomposite concentration

Mortality rate of worms is dose-dependent; in fact, it increases with the concentration. It was observed, Ag-MnO nanocomposites are more active than Mebendazole used as a positive control. The antihelmintic activity of Ag-MnO nanocomposites would be due to their capacity to create ROS in medium [33].

*3.7.Antioxidant activity*

Figure 9 below gives the evolution of inhibition rate of DPPH radical.

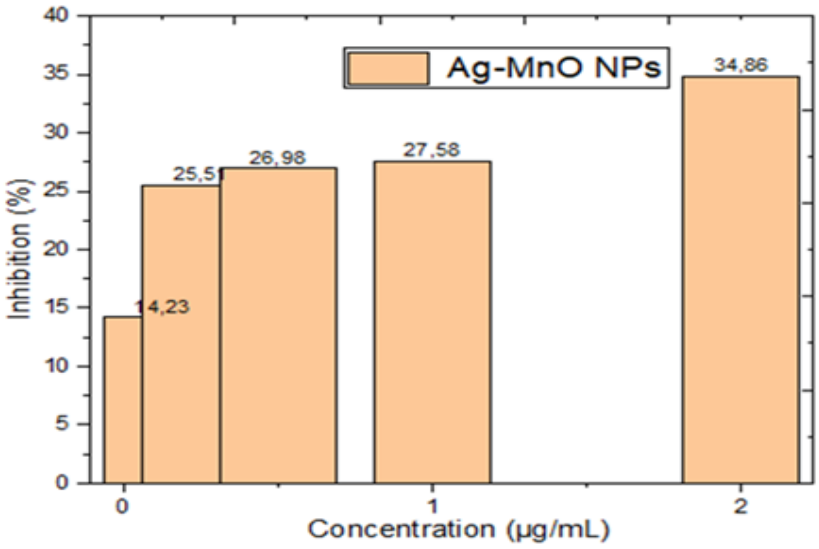


**Figure 9.** Inhibition rate of the DPPH radical by Ag-MnO nanocomposites.

Inhibition rate of DPPH radicals is dose-dependent. DPPH, a purple-colored free radical, is reduced to yellow-colored compound in the presence of scavenging compounds. However, the antioxidant activity of Ag-MnO nanocomposites would be due to the presence of secondary plant metabolites, which served for stabilization during the formation of these nanocomposites [35].

### *3.8.Anti-inflammatory activity*

The anti-inflammatory effect of nanocomposites was assessed in vitro against protein denaturation. Figure 10 below gives the rate of inhibition of the thermal denaturation of ovalbumin in vitro (%I) of Ag-MnO nanocomposites.

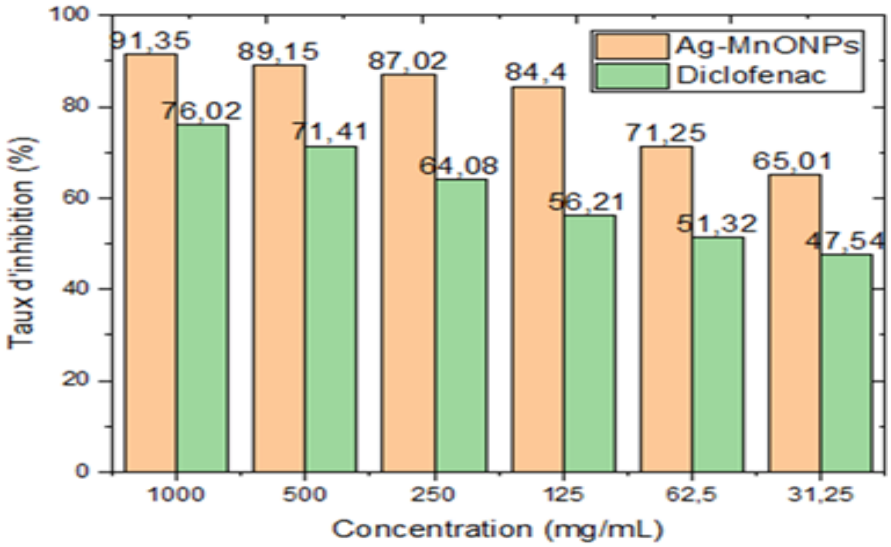


**Figure 10.** Percentage inhibition of protein denaturation (albumin)

The results showed concentration-dependent inhibition of protein denaturation by Ag-MnO nanocomposites. As it can be seen from the results in Figure 10, Ag-MnO nanocomposites exhibit anti-inflammatory activity. Ovalbumin thermal denaturation inhibition rates were 65.01%, 71.25%, 84.4%, 87.02%, 89.15%, and 91.35% for Ag-MnO nanocomposites at doses of 62.5 mg/mL, 31.25 mg/mL, 125 mg/mL, 250 mg/mL, 500 mg/mL, and 1000 mg/mL, respectively. Diclofenac sodium at the same doses as Ag-MnO NPs was used as a reference molecule, and the percentages of inhibition were respectively 47.54%, 51.32%, 56.21%, 64.08%, 71.41 %, and 76.02%. These results show that Ag-MnO nanocomposites anti-inflammatory effect is superior to that of diclofenac. Thus, the work of Jain and Priyanka based on silver nanopartcles reported an appreciable but lower anti-inflammatory effect compared to those proven by Ag-MnO nanocomposites. This may be due to the combination of manganese, which implies an additive effect [36,37].

### *3.9.Cytotoxicity*

Cytotoxicity was assessed using erythrocytes as a biological model. The extract is considered cytotoxic when, at 10 µg/mL, the hemolysis rate is ≥ 50%. It emerges from this study that the Ag-MnO nanocomposites are less hemolytic (% hemolysis = 6.49 1.089). It should, however, be noted that at 100 µg/mL, the hemolysis rate is less than 50%, which shows that Ag-MnO nanocomposites have no effect on hemolysis and can be used therapeutically.

## 4. Conclusions

The aim of the present study was to synthesize Ag-MnO nanocomposites from silver nitrate and manganese sulfate salts using the aqueous extract of *Cyttaranthus congolensis*

leaves and to evaluate their biological activities (antibacterial, antihelmintic, antioxidant, anti-inflammatory, and hemolytic). *Cyttaranthus congolensis* presented a good phytochemical profile, thin layer chromatography, and assay of secondary metabolites capable of reducing and stabilizing metals in nanoparticles were done.

These biosynthesized nanocomposites were characterized using several spectroscopic methods and exhibited good antibacterial, anti-inflammatory, antihelmintic and antioxidant properties and are non-hemotoxic. This confirms their potential to be used in therapy. Considering the negative impact of conventional nanoparticle synthesis methods, green synthesis is the best alternative for the synthesis of less toxic nanoparticles. This research leads to the development of a new cost-effective synthetic strategy and the reduction of chemical use in further studies. In perspective, so some points remain to be further investigated, so certain biological tests may be carried out with a view to exploiting other biological potentials of these new Ag-MnO materials.

## References

[1] T. Dodevska, I. Vasileva, P. Denev, D. Karashanova, B. Georgieva, D. Kovacheva, N. Yantcheva, A. Slavov, R. damascene. waste mediated synthesis of silver nanoparticles: Characteristics and application for an electrochemical sensing of hydrogen peroxide and vanillin, Materials Chemistry and Physics.; 231(2019)335-343. https://doi.org/10.1016/j.matchemphys.2019.04.030.

[2] N. Ahmad, F. indéfini, M. Jabeen, Z. Ul Haq, I. Ahmad, A. Wahab, Z.U. Islam, R. Ullah, A. Bari, M.A. Mohamed, F.M. El-Demerdash, M.K. Yahya. "Green Manufacture of silver nanoparticles using the aqueous extract of Euphorbia serpens Kunth, their characterization and the study of its antioxidant, antimicrobial, insecticidal and cytotoxic activities in vitro", BioMed Research International. 5562849 (2022) 11. https://doi.org/10.1155/2022/5562849.

[3] M. Ovais, A.T. Khalil, A. Raza, M.A. Khan, I. Ahmad, N.U. Islam, M. Saravanan, M.F. Ubaid, M. Ali, Z.K. Shinwari. Green synthesis of silver nanoparticles via plant extracts: beginning a new era in cancer theranostics. Nanomedicine (Lond). 11 (2016) 3157-3177. doi: 10.2217/nnm-2016-0279.

[4] Z. Fereshteh, M.R.L. Estarki, R.S. Razavi, M. Taheran. Template synthesis of zinc oxide nanoparticles entrapped in the zeolite Y matrix and applying them for thermal control paint, Materials Science in Semiconductor Processing. 16 (2013) 547-553. https://doi.org/10.1016/j.mssp.2012.08.005.

[5] Z.U.H. Khan, A. Khan, Y. Chen, N.S. Shah, N. Muhammad, A.U. Khan, K. Tahir, F.U. Khan, B. Murtaza, S.U. Hassan, S.A. Qaisrani, P. Wan. Biomedical applications of green synthesized Nobel metal nanoparticles, Journal of Photochemistry and Photobiology B: Biology. 173 (2017) 150-164. https://doi.org/10.1016/j.jphotobiol.2017.05.034.

[6] M. Rafique, I. Sadaf, M.S. Rafique, M.B. Tahir. A review on green synthesis of silver nanoparticles and their applications. Artif Cells Nanomed Biotechnol. 45 (2017) 1272-1291. doi: 10.1080/21691401.2016.1241792.

[7] A. Happy, M. Soumya, S.V. Kumar, S. Rajeshkumar, R.D. Sheba, T. Lakshmi, V.D. Nallaswamy. Phyto-assisted synthesis of zinc oxide nanoparticles using Cassia alata and its antibacterial activity against Escherichia coli, Biochemistry and Biophysics Reports. 17 (2019) 208-211. https://doi.org/10.1016/j.bbrep.2019.01.002.

[8] M. Herlekar, S. Barve, R. Kumar. "Synthèse verte médiée par les plantes de nanoparticules de fer", Journal of Nanoparticles. 9 (2014) 140614. https://doi.org/10.1155/2014/140614

[9] S. Ahmed, M. Ahmad, B.L. Swami, S. Ikram. A review on plants extracts mediated synthesis of silver nanoparticles for antimicrobial applications: A green expertise. J Adv Res. 7 (2016) 17-28. doi: 10.1016/j.jare.2015.02.007.

[10] G.K. Prashanth, P.A. Prashanth, U. Bora, M. Gadewar, B.M. Nagabhushana, S. Ananda, G.M. Krishnaiah, H.M. Sathyananda. In vitro antibacterial and cytotoxicity studies of ZnO nanopowders prepared by combustion assisted facile green synthesis, Karbala International Journal of Modern Science.1(2015) 67-77. https://doi.org/10.1016/j.kijoms.2015.10.007.

[11] M. Harshiny, M. Matheswaran, G. Arthanareeswaran, S. Kumaran, S. Rajasree. Enhancement of antibacterial properties of silver nanoparticles–ceftriaxone conjugate through Mukia maderaspatana leaf extract mediated synthesis, Ecotoxicology and Environmental Safety. 121(2015)135-141. https://doi.org/10.1016/j.ecoenv.2015.04.041.

[12] D.I. Pantelis, P.N. Karakizis, N.M. Daniolos, C.A. Charitidis, E.P. Koumoulos and D.A. Dragatogiannis. Microstructural study and mechanical properties of dissimilar AA5083-H111 and AA6082-T6 friction welds reinforced with SiC nanoparticles, materials and fabrication processes. 31 (2016) 264-274, DOI: 10.1080/10426914.2015.1019095

[13] T. Zohra, A.T. Khalil, F. Saeed, B. Latif, M. Salman, A. Ikram, M. Ayaz, H.C.A. Murthy. "Green Nano-Biotechnology: A New Sustainable Paradigm to Control Dengue Infection", Bioinorganic Chemistry and Applications. 3994340 (2022) 21. https://doi.org/10.1155/2022/3994340

[14] C.E. Lemaoui, H. Layaida, A. Badi, N. Foudi. Stratégies actuelles de lutte contre la résistance aux antibiotiques, Journal des Anti-infectieux. 19(2017)12-19. https://doi.org/10.1016/j.antinf.2017.01.003.

[15] D. Floresyona. Synthesis of Metal and Conjugated Polymer Nanostructures in Hexagonal Mesophases for Application in Fuel Cells and photocatalysis. Polymers. Paris Saclay University (COmUE). (2017). English. ⟨NNT: 2017SACLS206⟩. ⟨tel-01865813⟩

[16] J. Sourice. Synthesis of core-shell silicon-carbon nanocomposites by double-stage laser pyrolysis: application to the anode of lithium-ion batteries. Materials. Paris Sud University - Paris XI. (2015). French. ⟨NNT: 2015PA112166⟩. ⟨tel-01302856⟩

[17] N.M. El Fatah. Fabrication and characterization of Ag@AgCl nanocomposite thin films for photovoltaic applications. (2021). Doctoral thesis. http://hdl.handle.net/123456789/3350

[18] J.G. Mattei. Structure and chemical order in bimetallic nanoparticles: case of the Fe-Bi immiscible system. Materials Science [cond-mat.mtrl-sci]. Paul Sabatier University (Toulouse 3). (2012). French. ⟨NNT: 2012TOU30302⟩. ⟨tel-01937619⟩.

[19] E.M. Ngoyi, D.D. Tshilanda, J.T. Kilembe, E.M. Lengbiye, C.N. Kabengele, G.N. Kasiama, D.T.S. Tshibangu, D.O. Opota, K. Ngbolua, P.T. Mpiana. Phytochemical profile, antioxidant and anthelmintic activities of O. gratissimum leaves collected in Kinshasa (D.R. Congo). Discovery Phytomedicine.; 7(2020) 171-176. DOI: 10.15562/phytomedicine.

[20] G.N. Kasiama, A. Ikey, C.N. Kabengele, J.T. Kilembe, E.N. Matshimba, J.M. Bete, P.B. Bahati, C.L. Inkoto, P.K. Mutwale, K.N. Ngbolua, D.S.T. Tshibangu, D.D. Tshilanda and P.T. Mpiana*. Anthelmintic activity, antioxidant activity, phytochemical profile and microscopic features of Cassia alata collected in the Democratic Republic of Congo (DR Congo). 37(2022) 28-36; Article no.ARRB .87349. DOI: 10.9734/ARRB/2022/v37i630513

[21] K. Ngombe, F. Bukatuta, M. Kapepula, B. Moni, K. Makengo, L. Pambu, N. Bongo, M. Mbombo, M. Musuyu, U. Maloueki, N. Koto-Te-Nyiwa and F. Mbemba. Bioactivity and Nutritional values of some Dioscorea species traditionally used as Medicinal foods in Bandundu, DR congo, EJMP. 14(2016) 1-11, DOI: 10.9734/EJMP/2016/25124

[22] C.N. Kabengele, G.N .Kasiama, E.M. Ngoyi, C.L. Inkoto, J.M. Bete, P.B. Babady, D.S.T. Tshibangu, D.D. Tshilanda, H.M. Kalele, P.T. Mpiana, K. Ngbolua. Biogenic synthesis, characterization and effects of Mn-CuO composite nanocatalysts on Methylene blue photodegradation and Human erythrocytes[J]. AIMS Materials Science. 10(2023)356-369. doi: 10.3934/matersci.2023019

[23] S. Hatakeyama, Y. Ohama, M. Okazaki, Y. Nukui & K. Moriya. Test de sensibilité aux antimicrobiens de mycobactéries à croissance rapide isolées au Japon. BMC Infect Dis. 17 (2017).197. https://doi.org/10.1186/s12879-017-2298-8.

[24] C.N. Kabengele, E. M.Ngoyi, G.N. Kasiama, J.T. Kilembe, A. Matondo, C.L. Inkoto, E.M. Lengbiye, C.M. Mbadiko, J.J.D. Amogu, G.N. Bongo … P.T. Mpiana. Antihelminthic Activity, Phytochemical Profile and Microscopic Features of Ocimum basilicum Collected in DR Congo. AJOB. 10(2020) 42-50. DOI: 10.9734/AJOB/2020/v10i330110

[25] K.C. Sree, N. Yasmin, R.M. Hussain and M. Babuselvam. Invitro anti-inflammatory and anti-arthritic property of rhizopora mucronata leaves. International Journal of Pharma Sciences and Research (IJPSR). Flight.; 6 (2015) 3. ISSN: 0975-9492.

[26] A. Marina, D. Jeffrey, W. Barry, B. Jennifer, K. Anil and E. Scott. Method for Analysis of Nanoparticle Hemolytic Properties In Vitro. Nano Lett. 8(2009) 2180–2187. doi:10.1021/nl0805615.

[27] J.Y. Song et B.S. Kim. Synthèse biologique rapide de nanoparticules d'argent à l'aide d'extraits de feuilles de plantes. Bioprocess Biosyst Eng. 32(2009)79–84. https://doi.org/10.1007/s00449-008-0224-6

[28] S. Iravani. "Bacteria in Nanoparticle Synthesis: Current Status and Future Prospects", International Scholarly Research Notices. 18(2014) 359316. https://doi.org/10.1155/2014/359316

[29] M. Souri, V. Hoseinpour, N. Ghaemi and A. Shakeri. Optimisation de la procédure pour la synthèse verte de nanoparticules de dioxyde de manganèse par l'extrait de feuille de Yucca gloriosa. Int Nano Lett. 9(2019) 73–81. https://doi.org/10.1007/s40089-018-0257-z

[30] A. Khataee, M. Sheydaei, A. Hassani, M. Taseidifar and S. Karaca. Sonocatalytic removal of an organic dye using TiO2/montmoril lonite nanocomposite. Ultrasound. Sonochem. 22(2015)404–411. https://doi.org/10.1016/j.ultsonch.2014.07.002.

[31] Z. Alhalili. Green synthesis of copper oxide nanoparticles CuO NPs from Eucalyptus Globoulus leaf extract: Adsorption and design of experiments, Arabian Journal of Chemistry. 15(2022)1878-5352. https://doi.org/10.1016/j.arabjc.2022.103739.

[32] A. Nawaz, S. Bano, M. Yasir, A. Wadood and M.A. Rehman. Ag and Mn-doped mesoporous bioactive glass nanoparticles incorporated into the chitosan/ gelatin coatings deposited on PEEK/bioactive glass layers for favorable osteogenic differentiation and antibacterial activity. Mater. Adv. 1(2020) 1273-1284. DOI: 10.1039/d0ma00325e.

[33] H. Xu. Elaboration of laccase T. cross-linked ultraporous aluminas for Remazol Brilliant Blue R removal. Material chemistry. Université Paris-Nord - Paris XIII. (2021) English. ⟨NNT: 2021PA131076⟩. ⟨tel-03886067⟩

[34] M.H. Yap, K.L. Fow, G.Z. Chen. Synthesis and applications of MOF-derived porous nanostructures, Green Energy & Environment.; 2(2017)218-245. https://doi.org/10.1016/j.gee.2017.05.003.

[35] M.H. El-Rafie and M.A. Hamed. Antioxidant and anti-inflammatory activities of silver nanoparticles biosynthesized from aqueous leaves extracts of four Terminalia species. Adv. Nat. Sci: Nanosci. Nanotechnology.; 5(2014)035008. DOI 10.1088/2043-6262/5/3/035008.

[36] J. Aditya, A. Roy, S. Rajeshkumar. Anti-inflammatory activity of silver nanoparticles synthesized using cumin oil. Research Journal of Pharmacy and Technology.); 12(2019)2790-2793; DOI: 10.5958/0974-360X.2019.00469.4

[37] P. Singh, S. Ahn, J.P. Kang, S. Veronika, Y. Huo, H. Singh, M. Chokkaligam, F.M. Agamy, V.C. Aceituno, Y.J. Kim, D.C. Yang. In vitro anti-inflammatory activity of spherical silver nanoparticles and monodisperse hexagonal gold nanoparticles by fruit extract of Prunus serrulata: a green synthetic approach. Artif Cells Nanomed Biotechnol. 46(2018)2022-2032. doi: 10.1080/21691401.2017.1408117.